Synthesis and Reactivity of Group 4 Homoleptic Selenolates and Tellurolates: Lewis Base Induced Conversion to Terminal and Bridging Chalcogenides

Christopher P. Gerlach, Victor Christou, and John Arnold*

Department of Chemistry, University of California, Berkeley, California 94720

Received January 19, 1996[⊗]

A combination of either salt metathesis reactions between MCl_4 (M = Zr, Hf) and $(THF)_2LiSeSi(SiMe_3)_3$ (THF = tetrahydrofuran) or between $TiCl_3(THF)_3$ and $(THF)_2LiESi(SiME_3)_3$ (E = Se, Te), or chalcogenolysis reactions between $M(CH_2Ph)_4$ (M = Zr, Hf) and $HESi(SiMe_3)_3$ (E = Se, Te) afforded the series of compounds $M[ESi(SiMe_3)_3]_4$ (M = Ti, Zr, Hf; E = Se, Te). The X-ray structures of $M[TeSi(SiMe_3)_3]_4$ (M = Zr, Hf) and $Zr[SeSi(SiMe_3)_3]_4$ have been determined and are presented for comparison. Reaction of group 4 tetrabenzyls with 3 equiv of $HSeSi(SiMe_3)_3$ gave the complexes $M[SeSi(SiMe_3)_3]_3(CH_2Ph)$ (M = Ti, Zr, Hf) in high yields. Treatment of the zirconium and hafnium homoleptic tellurolates with 2 equiv of xylyl isocyanide produced the bis-L trans adducts $M[TeSi(SiMe_3)_3]_4[CN(xylyl)]_2$ (M = Zr, Hf) in moderate yields. The related six-coordinate DMPE adducts $M[TeSi(SiMe_3)_3]_4$(DMPE) (M = Zr, Hf; DMPE = 1,2-bis(dimethylphosphino)ethane) were similarly prepared. Reaction of the mono-DMPE complexes with a second equilvalent of DMPE led to the elimination of $Te[Si(SiMe_3)_3]_2$ and the formation of the seven-coordinate bis(tellurolate), bis(DMPE), terminal tellurides $M[TeSi(SiMe_3)_3]_2(Te)(DMPE)_2$ (M = Zr, Hf). Both of the tellurides have been structurally characterized. The homoleptic zirconium selenolate reacts with 1 equiv of DMPE, yielding a bright red material with the stoichiometry $Zr[SeSi(SiMe_3)_3]_2(Se)$(DMPE). The diphosphine DMPM (DMPM = 1,2-bis(dimethylphosphino)methane) also reacted with $M[SeSi(SiMe_3)_3]_4$ (M = Zr, Hf) to give the bis(μ-Se), A-frame dimers $\{M[SeSi(SiMe_3)_3]_2(\mu\text{-Se})(\mu\text{-}\eta^2\text{-DMPM})\}_2$ (M = Zr, Hf) in relatively low yields (40 and 23%). The structure of the zirconium derivative has been confirmed using X-ray crystallography. Crystallographic data are as follows: $Zr[SeSi(SiMe_3)_3]_4$, monoclinic, $P2_1/c$, a = 22.6944(34) Å, b = 15.2943(55) Å, c = 22.7758(61) Å, β = 105.695(17)°, Z = 4, R = 5.29, R_w = 3.69; $Hf[TeSi(SiMe_3)_3]_4$, monoclinic, $P2_1/c$, a = 22.494(5) Å, b = 15.609(5) Å, c = 22.742(5) Å, β = 104.480(5)°, Z = 4, R = 4.48, R_w = 5.45; $Hf[TeSi(SiMe_3)_3]_2(Te)(DMPE)_2$, monoclinic, $P2_1$, a = 14.795(3) Å, b = 14.289(3) Å, c = 15.4212(2) Å, β = 102.543(3)°, Z = 2, R = 4.78, R_w = 6.70; $\{Zr[SeSi(SiMe_3)_3]_2(\mu\text{-Se})(\mu\text{-}\eta^2\text{-DMPM})\}_2$, monoclinic, $P2_1/n$, a = 14.7651(13) Å, b = 18.8579(17) Å, c = 18.6072(17) Å, β = 111.031(1)°, Z = 2, R = 8.26, R_w = 8.13.

Introduction

The synthesis of transition metal and main group chalcogenolates containing the heavier members of group 16 has expanded in recent years with the use of bulky ligands that stabilize low-coordinate and low-molecularity compounds.[1,2] Our efforts have concentrated on the synthesis of complexes with bulky alkyl- and silylchalcogenolate ligands $-EX(SiMe_3)_3$ (E = S, Se, Te; X = C, Si), and we have reported an extensive range of derivatives involving transition metal,[3−7] rare earth,[8−10] and main group elements.[11−14]

We have found that reaction of metal chalcogenolate complexes with donor ligands may result in the elimination of dialkyl- or disilylchalcogenide (ER_2) and formation of soluble metal chalcogenides.[6,15] These reactions offer novel routes toward metal chalcogenides and may be regarded as homogenous, solution state models for related eliminations that lead to the formation of solid-state materials (eq 1).[16] While recent

$$M(ER)_2 \rightarrow [ME]_n + ER_2 \quad (1)$$
$$E = S, Se, Te$$
$$R = alkyl, silyl, aryl$$

mechanistic studies have begun to shed light on chalcogenolate-to-chalcogenide transformations,[17−19] there still is much to be

[⊗] Abstract published in *Advance ACS Abstracts,* April 1, 1996.

(1) Arnold, J. In *Progress in Inorganic Chemistry*; Karlin, K. D., Ed.; John Wiley & Sons: New York, 1995; Vol. 43, p 353.
(2) See the following and references cited therein for recent examples of metal selenolates and tellurolates: Ellison, J. J.; Ruhlandt-Senge, K.; Hope, H. H.; Power, P. P. *Inorg. Chem.* **1995**, *34*, 49. MacDonnell, F. M.; Ruhlandt-Senge, K.; Ellison, J. J.; Holm, R. H.; Power, P. P. *Inorg. Chem.* **1995**, *34*, 1815. Wehmschulte, R. J.; Ruhlandt-Senge, K.; Power, P. P. *Inorg. Chem.* **1995**, *34*, 2593. Liaw, W. F.; Ou, D. S.; Li, Y. S.; Lee, W. Z.;Chuang, C. Y.; Lee, Y. P.; Lee, G. H.; Peng, S. M. *Inorg. Chem.* **1995**, *34*, 3747. Gardiner, M. G.; Raston, C. L.; Tolhurst, V. A. *J. Chem. Soc., Chem. Commun.* **1995**, 1457. Brewer, M.; Khasnis, D.; Buretea, M.; Berardini, M.; Emge, T. J.; Brennan, J. G. *Inorg. Chem.* **1994**, *33*, 2743−2747. Khasnis, D. V.; Brewer, M.; Lee, J.; Emge, T. J.; Brennan, J. G. *J. Am. Chem. Soc.* **1994**, *116*, 7129. Bochmann, M.; Bwembya, G. C.; Grinter, R.; Powell, A. K.; Webb, K. J.; Hursthouse, M. B.; Malik, K. M. A.; Mazid, M. A. *Inorg. Chem.* **1994**, *33*, 2290. Strzelecki, A. R.; Likar, C. L.; Helsel, B. A.; Utz, T.; Lin, M. C.; Bianconi, P. A. *Inorg. Chem.* **1994**, *33*, 5188. Labahn, D.; Bohnen, F. M.; Herbst-Irmer, R.; Pohl, E.; Stalke, D.; Roesky, H. W. *Z. Anorg. Allg. Chem.* **1994**, *620*, 41. Bonasia, P. J.; Arnold, J. *J. Organomet. Chem.* **1993**, *449*, 147.
(3) Gindelberger, D. E.; Arnold, J. *Inorg. Chem.* **1994**, *33*, 6293.
(4) Gindelberger, D. E.; Arnold, J. *Inorg. Chem.* **1993**, *32*, 5813.
(5) Christou, V.; Wuller, S. P.; Arnold, J. *J. Am. Chem. Soc.* **1993**, *115*, 10545.
(6) Christou, V.; Arnold, J. *J. Am. Chem. Soc.* **1992**, *114*, 6240.
(7) Bonasia, P. J.; Christou, V.; Arnold, J. *J. Am. Chem. Soc.* **1993**, *115*, 6777.
(8) Cary, D. R.; Ball, G. E.; Arnold, J. *J. Am. Chem. Soc.* **1995**, *117*, 3492.
(9) Cary, D. R.; Arnold, J. *Inorg. Chem.* **1994**, *33*, 1791.
(10) Cary, D. R.; Arnold, J. *J. Am. Chem. Soc.* **1993**, *115*, 2520.
(11) Bonasia, P. J.; Gindelberger, D. E.; Arnold, J. *Inorg. Chem.* **1993**, *32*, 5126.
(12) Bonasia, P. J.; Mitchell, G. P.; Hollander, F. J.; Arnold, J. *Inorg. Chem.* **1994**, *33*, 1797.
(13) Seligson, A. L.; Arnold, J. *J. Am. Chem. Soc.* **1993**, *115*, 8214.
(14) Bonasia, P. J.; Arnold, J. *Inorg. Chem.* **1992**, *31*, 2508.
(15) Christou, V.; Arnold, J. *Angew. Chem., Int. Ed. Engl.* **1993**, *32*, 1450.

S0020-1669(96)00068-7 CCC: $12.00

learned. Since molecular species may be used as precursors for technologically important solids such as II/VI materials,[20−22] detailed knowledge of the factors governing reactions similar to that shown in eq 1[23,24] is important for the development of appropriate reagents.

Here we report the synthesis of $M[ESi(SiMe_3)_3]_4$ and $M[SeSi(SiMe_3)_3]_3(CH_2Ph)$ (M = Ti, Zr, Hf; E = Se, Te). The X-ray crystal structures of the zirconium and hafnium tellurolates and the zirconium homoleptic selenolate have been determined. Conversion of the tellurolates to the novel terminal tellurides $M[TeSi(SiMe_3)_3]_2(Te)(DMPE)_2$ (DMPE = 1,2-bis(dimethylphosphino)ethane) (M = Zr, Hf) is also reported, and the crystallographic characterization of these products offers the unique opportunity to compare the bond lengths of singly and doubly bonded tellurium to a single metal center. The synthesis of $\{M[SeSi(SiMe_3)_3]_2(\mu\text{-Se})(\mu\text{-DMPM})\}_2$ (DMPM = 1,2-bis(dimethylphosphino)methane) (M = Zr, Hf) and X-ray structure of the zirconium complex are also described. Except for a report in 1970 of homoleptic −SePh derivatives,[25] selenolates and tellurolates of group 4 metals without cyclopentadienyl supporting ligands are unknown. Preliminary aspects of this work were described earlier.[6]

Results and Discussion

Group 4 Selenolates and Tellurolates. A combination of either salt metathesis or chalcogenolysis reactions were successful in preparing the complete series of group 4 homoleptic tris(trimethylsilyl)silyl selenolates and tellurolates, as summarized in eqs 2−4.

$$MCl_4 + 4(THF)_2LiSeSi(SiMe_3)_3 \rightarrow M[SeSi(SiMe_3)_3]_4 \quad M = Zr, Hf \tag{2}$$

$$M(CH_2Ph)_4 + 4HESi(SiMe_3)_3 \rightarrow M[ESi(SiMe_3)_3]_4 \quad M = Zr, Hf;\ E = Se, Te \tag{3}$$

$$TiCl_3(THF)_3 + 3(THF)_2LiESi(SiMe_3)_3 \rightarrow Ti[ESi(SiMe_3)_3]_4 + ... \quad E = Se, Te \tag{4}$$

Related reactions between $TiCl_4(THF)_2$ and $(THF)_2LiSeSi(SiMe_3)_3$ or $TiCl_4(NC_5H_5)_2$ and $Mg[TeSi(SiMe_3)_3]_2$[3] also gave the homoleptic titanium derivatives, but the reactions appeared to be complex and yields were erratic. Although the reaction in eq 4 apparently involves disproportionation of titanium(III), no lower valent titanium species could be separated from the mixture and attempts at trapping the putative $Ti[ESi(SiMe_3)_3]_3$ intermediate with phosphines or carbon monoxide were not successful. We note that the related reaction between $Ti[N(SiMe_3)_2]_3$ and 3 equiv of 2,6-$(i\text{-}Pr)_2C_6H_3OH$ yields the homoleptic titanium(IV) aryloxide, presumably by a similar pathway.[26]

Table 1. Selected Physical and Spectroscopic Data

compound	color	mp (dec) (°C)	$^{77}Se/^{125}Te$ NMR (δ)
$Ti[SeSi(SiMe_3)_3]_4$	black	261−263	865
$Zr[SeSi(SiMe_3)_3]_4$	orange	268−269	356
$Hf[SeSi(SiMe_3)_3]_4$	yellow	262−264	211
$Ti[TeSi(SiMe_3)_3]_4$	black	230−232	1302
$Zr[TeSi(SiMe_3)_3]_4$	green	227−230	459
$Hf[TeSi(SiMe_3)_3]_4$	red	225−230	193
$Ti[SeSi(SiMe_3)_3]_3(CH_2Ph)$	rust	174−176	828
$Zr[SeSi(SiMe_3)_3]_3(CH_2Ph)$	bright orange	172−174	338
$Hf[SeSi(SiMe_3)_3]_3(CH_2Ph)$	light yellow	172−178	206

Physical properties and spectroscopic data for selected compounds are collected in Table 1. All of the tellurolates may be crystallized from hexanes; however, the more soluble selenolates are best obtained by crystallization from hexamethyldisiloxane (HMDSO). In the titanium case, the mono-HMDSO solvate was always obtained. In contrast to the tellurolates, the homoleptic selenolates do not decompose when exposed to dry oxygen for short periods in the solid state or in solution (C_6D_6); however, all of these derivatives are moisture sensitive. The titanium and hafnium homoleptic tellurolates are mildly photosensitive in solution. In the solid state, slight surface decomposition appears to half further reaction since the materials remain spectroscopically pure. Inspection of the ^{77}Se and ^{125}Te NMR data shows the typical upfield progression in chemical shifts as the central metal atom becomes heavier.[17] The values for the homoleptic tellurolates are each 400−500 ppm downfield from related values in the more electron rich species $Cp_2M[TeSi(SiMe_3)_3]_2$ (M = Ti, Zr, Hf).[5]

The X-ray crystal structures of $Zr[TeSi(SiMe_3)_3]_4$ and $Hf[TeSi(SiMe_3)_3]_4$ have been determined. Details on the Zr derivative were communicated earlier,[6] and the metrical parameters of the Hf analogue are, as expected, very similar. A view of the Hf complex is provided in Figure 1, and selected bond lengths and bond angles are given in Table 2. The Hf−Te−Si angles average 118.8(1)°, while the Te−Hf−Te angles vary widely from 101.73(3) to 116.28(3)°. The tetrahedral symmetry is distorted such that two of the six angles are significantly larger than the remaining four (Te1−Hf−Te4 = 115.78(3)°; Te2−Hf−Te3 = 116.28(3)°). A similar distortion occurs in the solid state structures of $Zr[TeSi(SiMe_3)_3]_4$ and $Ti[S\text{-}2,3,5,6\text{-}Me_4C_6H]_4$.[27] The Hf−Te bond lengths (2.707(1)−2.731(1) Å) are well-estimated by the sum of the covaent radii (Hf = 1.48 Å; Te = 1.36 Å)[28] once the value is corrected for ionic shortening (−0.072 Å) by the Schomaker−Stevenson

(16) For recent examples, see the following and references cited therein: Cheng, Y.; Emge, T. J.; Brennan, J. G. *Inorg. Chem.* **1994**, *33*, 3711. Coleman, A. P.; Dickson, R. S.; Deacon, G. B.; Fallon, G. D.; Ke, M.; McGregor, K.; West, B. O. *Polyhedron* **1994**, *13*, 1277. Seligson, A. L.; Bonasia, P. J.; Arnold, J.; Yu, K.-M.; Walker, J. M.; Bourret, E. D. *Mat. Res. Soc. Symp. Proc.* **1993**, *282*, 665. Bochmann, M.; Webb, K. J. *J. Chem. Soc., Dalton Trans.* **1991**, 2325. Bochmann, M.; Webb, K. J.; Hursthouse, M. B.; Mazid, M. *J. Chem. Soc., Dalton Trans.* **1991**, 2317. Brennan, J. G.; Siegrist, T.; Carroll, P. J.; Stuczynski, S. M.; Reynders, P.; Brus, L. E.; Steigerwald, M. L. *Chem. Mater.* **1990**, *2*, 403.
(17) Gindelberger, D. E.; Arnold, J. *Organometallics* **1994**, *13*, 4462.
(18) Piers, W. E. *J. Chem. Soc., Chem. Commun.* **1994**, 309.
(19) Piers, W. E.; Parks, D. J.; MacGillivray, L. R.; Zaworotko, M. J. *Organometallics* **1994**, *13*, 4547.
(20) Colvin, V. L.; Schlamp, M. C.; Alivisatos, A. P. *Nature* **1994**, *370*, 354.
(21) Hoheisel, W.; Colvin, V. L.; Johnson, C. S.; Alivisatos, A. P. *J. Chem. Phys.* **1994**, *101*, 8455.
(22) O'Brien, P. *Chemtronics* **1991**, *5*, 61.
(23) Steigerwald, M. L.; Siegrist, T.; Gyorgy, E. M.; Hessen, B.; Kwon, Y. U.; Tanzler, S. M. *Inorg. Chem.* **1994**, *33*, 3389.
(24) Steigerwald, M. L. *Polyhedron* **1994**, *13*, 1245.
(25) Andra, K. *Z. Anorg. Allg. Chem.* **1970**, *373*, 209.
(26) Minhas, R.; Duchateau, R.; Gambarotta, S.; Bensimon, C. *Inorg. Chem.* **1992**, *31*, 4933.
(27) Corwin, D. T. J.; Corning, J. F.; Koch, S. A.; Millar, M. *Inorg. Chim. Acta* **1995**, *229*, 335.
(28) The covalent radii of Zr (1.50 Å) and Hf (1.48 Å) were estimated by substracting the covalent radius of carbon (0.77 Å) from the average M−C bond lengths in the tetrabenzyls. The covalent radius of Te (1.36 Å) and Se (1.16 Å) were calculated from structural data for $-ESi(SiMe_3)_3$ over a range of crystallographically characterized tellurolate and selenolate complexes (for the crystal structures of $Zr(CH_2Ph)_4$ and $Hf(CH_2Ph)_4$, respectively, see: Davies, G. R.; Jarvis, J. A. J.; Kilbourn, B. T.; Pioli, J. P. *J. Chem. Soc., Chem. Commun.* **1971**, 677. Davies, G. R.; Jarvis, J. A. J.; Kilbourn, B. T. *J. Chem. Soc., Chem. Commun.* **1971**, 1511).

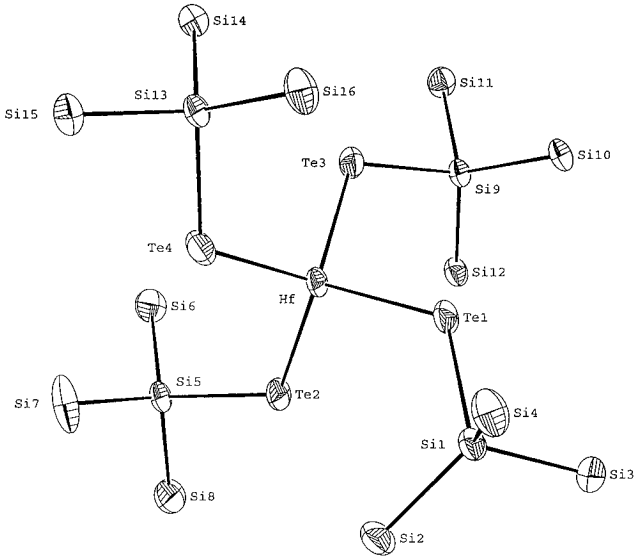

Figure 1. ORTEP view of the molecular structure of Hf[TeSi(SiMe$_3$)$_3$]$_4$. Methyl groups are omitted for clarity. Thermal ellipsoids are plotted at the 50% probability level.

Table 2. Selected Metrical Parameters for Hf[TeSi(SiMe$_3$)$_3$]$_4$ and Zr[SeSi(SiMe$_3$)$_3$]$_4$

Hf[TeSi(SiMe$_3$)$_3$]$_4$		Zr[SeSi(SiMe$_3$)$_3$]$_4$	
Bond Distances (Å)			
Hf−Te1	2.7068(8)	Zr−Se(1)	2.516(2)
Hf−Te2	2.7311(8)	Zr−Se(2)	2.522(2)
Hf−Te3	2.7165(8)	Zr−Se(3)	2.514(2)
Hf−Te4	2.7121(9)	Zr−Se(4)	2.536(2)
Te−Si$_{av}$	2.534(3)	Se−Si$_{av}$	2.323(6)
Bond Angles (deg)			
Hf−Te1−Si1	123.57(7)	Zr−Se1−Si1	126.19(9)
Hf−Te2−Si5	119.66(8)	Zr−Se2−Si5	119.35(8)
Hf−Te3−Si9	114.55(7)	Zr−Se3−Si9	123.72(9)
Hf−Te4−Si13	117.61(7)	Zr−Se4−Si13	126.29(9)
Te1−Hf−Te2	107.80(3)	Se1−Zr−Se2	103.67(5)
Te1−Hf−Te3	101.73(3)	Se1−Zr−Se3	114.89(6)
Te1−Hf−Te4	115.78(3)	Se1−Zr−Se4	107.86(5)
Te2−Hf−Te3	116.28(3)	Se2−Zr−Se3	106.88(5)
Te2−Hf−Te4	108.22(3)	Se2−Zr−Se4	114.85(5)
Te3−Hf−Te4	107.25(3)	Se3−Zr−Se4	108.84(5)

equation.[29] Nevertheless, the observed distances are slightly shorter (0.04−0.06 Å) and may be indicative of some multiple bond character. In this regard, it is interesting to note that recent X_α calculations of the bonding in the model complex Zr(TeSiH$_3$)$_4$ predict that the π-symmetry MOs constructed from the tellurium 5p orbitals and the zirconium d orbitals are approximately one-third metal d in character. While π-interactions between the heavier chalcogens and early transition metals have typically been thought of as relatively weak, clearly they are likely to be more favored in cases where the metal is severely electron deficient (i.e. formally eight electrons in M(ER)$_4$).

An ORTEP view of Zr[SeSi(SiMe$_3$)$_3$]$_4$ is shown in Figure 2, and selected bond lengths and angles are given in Table 2. The structure consists of well-separated molecules with the zirconium coordinated by the four selenium atoms in a pseudo-tetrahedral fashion. The sum of covalent radii (2.66 Å) corrected for ionic shortening (−0.10 Å) gives a predicted value of 2.56 Å for the Zr−Se bond distances. The observed bond lengths of 2.514(1)−2.522(2) Å are thus about 0.04 Å shorter, again possibly due to multiple bond character. The range of Se−Zr−Se angles (103.67(5)−114.89(6)°) indicates a similar distortion from

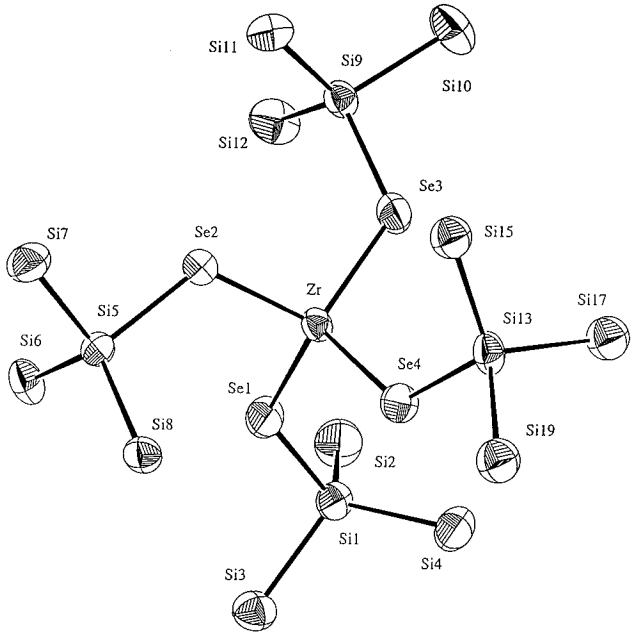

Figure 2. ORTEP view of the molecular structure of Zr[SeSi(SiMe$_3$)$_3$]$_4$. Methyl groups are omitted for clarity. Thermal ellipsoids are plotted at the 50% probability level.

tetrahedral symmetry as in the tellurolates. The average of the Zr−Se−Si angles (123.9(2)°) is greater than the average of the M−Te−Si angles in Zr[TeSi(SiMe$_3$)$_3$]$_4$ (119.24(5)°) and Hf[TeSi(SiMe$_3$)$_3$]$_4$ (118.8(1)°) and is presumably due to the larger steric requirement of the −SeSi(SiMe$_3$)$_3$ ligand due to the shorter Zr−Se and Se−Si bond lengths.

Reaction of the group 4 homoleptic benzyls with 3 equiv of HSeSi(SiMe$_3$)$_3$ afforded the tris(selenolates) in high yields (eq 5). Generally, the reactions were quite clean, although the Zr

$$M(CH_2Ph)_4 + 3HSeSi(SiMe_3)_3 \rightarrow M[SeSi(SiMe_3)_3]_3(CH_2Ph) \quad M = Ti, Zr, Hf \tag{5}$$

derivative was always contaminated with a small amount of the tetraselenolate (ca. 5%). Analogous reactions with HTeSi(SiMe$_3$)$_3$ were not as selective due to its higher reactivity as compared to the selenol. The benzyl groups are bound in a normal η^1-fashion as evidenced by the downfield resonances of the ortho protons in their ^{1}H NMR spectra and the absence of low-energy ν_{CH} in the IR spectrum.[31,32] The compounds have nearly identical melting (decomposition) points that are lower than those observed for the homoleptic selenolates (Table 1). The ^{77}Se NMR spectra possess singlets that are all shifted upfield from the values of the resonances observed in the homoleptic selenolates. Nevertheless, the upfield progression of the chemical shifts as the atomic number of the central metal atom increases mirrors the trend observed within their homoleptic counterparts (Table 1). The chemical shifts of heavy nuclei are strongly influenced by low-energy, electronic excited states[33] such that compounds with higher-energy (visible) absorptions display higher-field NMR shifts and vice versa.[17] Thus, as expected, the lowest-energy absorptions in the electronic spectra

(29) Schomaker, V.; Stevenson, D. P. *J. Am. Chem. Soc.* **1941**, *63*, 37.
(30) Kaltsoyannis, N. *J. Chem. Soc., Dalton Trans.* **1994**, 1391.
(31) Jordan, R. F.; LaPointe, R. E.; Bradley, P. K.; Baenziger, N. *Organometallics* **1989**, *8*, 2892.
(32) Jordan, R. F.; LaPointe, R. E.; Baenziger, N.; Hinch, G. D. *Organometallics* **1990**, *9*, 1539.
(33) Karplus, M.; Pople, J. A. *J. Chem. Phys.* **1963**, *38*, 2803.

of the $M[SeSi(SiMe_3)_3]_3(CH_2Ph)$ complexes are blue-shifted compared to those in the analogous tetraselenolates.[34]

Attempts to prepare mixed chalcogenolate compounds by reactions of $Zr[SeSi(SiMe_3)_3]_4$ with 2 equiv of alcohol or phenol resulted in complete alcoholysis (eq 6). These reactions were

$$Zr(SeR)_4 + 2R'OH \rightarrow {}^1/_2Zr(SeR)_4 + {}^1/_2Zr(OR')_4 + 2HSeR$$
$$R = Si(SiMe_3)_3;\ R' = Me,\ Bu^t,\ 2,6\text{-}Pr^i{}_2C_6H_3 \qquad (6)$$

quantitative as judged by ^1H NMR spectroscopy and no $M(SeR)_{4-x}(OR')_x$ species were detected. The identities of the alkoxides were verified by comparison of spectroscopic data to literature values. Alcoholysis with 1 equiv of catechol proceeded analogously, but the sterically encumbered phenol $2,6\text{-}Bu^t{}_2C_6H_3OH$ did not react, even after prolonged heating.

The alkoxide−selenolate $Ti[SeSi(SiMe_3)_3]_2(OEt)_2$ was produced by heating a C_7D_8 solution of $Ti(CH_2Ph)_2(OEt)_2$[35] with 2 equiv of $HSeSi(SiMe_3)_3$ (eq 7). The product is stable in

$$Ti(CH_2Ph)_2(OEt)_2 + 2HSeSi(SiMe_3)_3 \rightarrow Ti[SeSi(SiMe_3)_3]_2(OEt)_2 \qquad (7)$$

solution over days at room temperature but appears to decompose on concentration of the reaction solution, and we have been unable to isolate it in pure form. Interestingly, while $Ti(CH_2Ph)_2(OEt)_2$ exists as a dimer with bridging and terminal ethoxide groups in both the solid state[36] and in solution,[35] variable temperature NMR studies showed a single environment for each set of ligands down to −90 °C. These results are consistent with the compound being monomeric, though an oligomeric species whose bridging and terminal ligands are exchanging rapidly on the NMR time scale cannot be ruled out. The selenium nuclei are more shielded than in $Ti[SeSi(SiMe_3)_3]_4$ (δ 416 versus δ 865 in the latter), most likely due to the higher π-donating effect of the ethoxide groups.

Reactions of M[ESi(SiMe$_3$)$_3$]$_4$ with Lewis Bases. Despite the steric shielding of the four bulky tellurolate ligands, the coordinatively and electronically unsaturated $M[TeSi(SiMe_3)_3]_4$ compounds readily interact with small two-electron donors. For example, $Zr[TeSi(SiMe_3)_3]_4$ forms a red-brown adduct with 1,2-dimethoxyethane (DME), as well as purple, trans L_2 adducts with PMe_3 and pyridine. The six-coordinate, bis(xylylisocyanide) complexes $M[TeSi(SiMe_3)_3]_4(CN(xylyl))_2$ (M = Zr, 70%; M = Hf, 49%) have been isolated and fully characterized (eq 8). Chemically equivalent tellurolate ligands suggest a trans

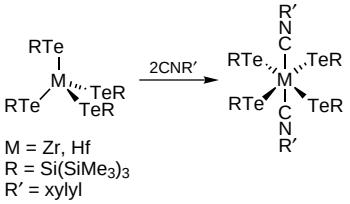

(8)

disposition of the isocyanide ligands in solution, and the observance of a single ν_{CN} in their IR spectra (2151 and 2153 cm^{-1}) implies a similar structure in the solid state. In all of the base adducts, the ^{125}Te NMR signals are shifted upfield from their values in the homoleptic species.

Table 3. Selected Metrical Parameters for $Hf[TeSi(SiMe_3)_3]_2(Te)(DMPE)_2$

Bond Distances (Å)			
Hf−Te1	3.019(1)	Hf−P_{av}	2.769(8)
Hf−Te2	2.918(2)	Te1−Si1	2.525(6)
Hf−Te3	2.637(2)	Te2−Si5	2.521(6)
Bond Angles (deg)			
Te1−Hf−Te2	86.05(4)	Te1−Hf−P2	71.5(3)
Te1−Hf−Te3	105.31(5)	Te1−Hf−P4	74.6(4)
Te2−Hf−Te3	168.51(6)	P1−Hf−P3	74.2(3)
P1−Hf−P2	70.6(5)	Hf−Te1−Si1	128.26(14)
P3−Hf−P4	69.2(6)	Hf−Te2−Si5	142.31(16)

A 1 equiv amount of DMPE also reacts with the zirconium and hafnium tellurolates, forming related six-coordinate, cis adducts (eq 9). The compounds were isolated from hexanes as

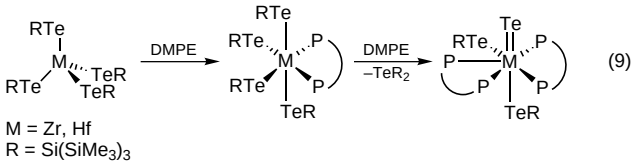

(9)

maroon (Zr) and bronze (Hf) colored solids. The observation of two singlets for the $-TeSi(SiMe_3)_3$ ligands in both the ^1H and ^{125}Te NMR spectra is consistent with a six-coordinate, η^2-DMPE complex, however, the broad linewidth of the latter signals prevented the resolution of any $^2J_{TeP}$. Singlets at δ −2.92 (Zr) and δ −3.36 (Hf) are observed in the $^{31}P\{^1H\}$ NMR for the chemically equivalent phosphorous nuclei.

Reaction with a second equivalent of DMPE results in the elimination of disilyltelluride and the formation of terminal telluride−bis(tellurolates) (eq 9) in good yields. The red-brown compounds were isolated as crystalline solids from hexanes (Zr, 86%; Hf, 55%), with the hafnium derivative being slightly photosensitive in solution and the solid state. As expected for seven-coordinate species, variable temperature NMR experiments showed evidence for stereochemical nonrigidity in toluene at room temperature. At −80 °C, the terminal telluride ligands are characterized by ^{125}Te signals at δ −706 and δ −701 for the zirconium and hafnium derivatives, respectively. Interestingly, these values are significantly upfield from those reported for terminal tellurides of groups 5[15,37] and 6.[38,39] The tellurium nuclei of the tellurolate ligands are also highly shielded (δ −1173, −1197 for Zr; δ −1212, −1250 for Hf) relaive to the four-coordinate homoleptics. Although the phosphorous nuclei make up an AA′BB′ spin system, the magnetic inequivalence is not resolved at low temperature (−80 °C) and two broad singlets are observed in the $^{31}P\{^1H\}$ NMR spectrum of each compound. Similarly, in the ^1H NMR spectra, the DMPE methyl and methylene hydrogens give rise to two signals each.

The crystal structures of $M[TeSi(SiMe_3)_3]_2(Te)(DMPE)_2$ (M = Zr, Hf) have been determined with structural details on the Zr derivative communicated earlier.[6] Selected metrical parameters for the Hf compound are given in Table 3 and an ORTEP view in Figure 3. Except for slightly shorter Hf−ligand bond lengths, the structures are very similar. The seven-coordinate molecules are well-approximated as pentagonal bipyramids with the DMPE phosphorous atoms and the Te of a tellurolate in the pentagonal belt, and the doubly bonded telluride and remaining tellurolate coordinated at the apices. The Hf−Te−Si angles (Hf−Te1−Si1 = 128.26(14)°; Hf−Te2−Si5 = 142.31(16)°) are at the high end of those observed for metal

(34) For a similar correlation in ^{13}C NMR spectroscopy, see: Breitmaier, E.; Voelter, W. *Carbon-13 NMR Spectroscopy*; VCH: New York, 1987, p 110.
(35) Zucchini, U.; Albizzati, E.; Giannini, U. *J. Organomet. Chem.* **1971**, *26*, 357.
(36) Stoeckli-Evans, H. *Helv. Chim. Acta* **1975**, *58*, 373.
(37) Shin, J. H.; Parkin, G. *Organometallics* **1994**, *13*, 2147.
(38) Murphy, V. J.; Parkin, G. *J. Am. Chem. Soc.* **1995**, *117*, 3522.
(39) Rabinovich, D.; Parkin, G. *J. Am. Chem. Soc.* **1991**, *113*, 9421.

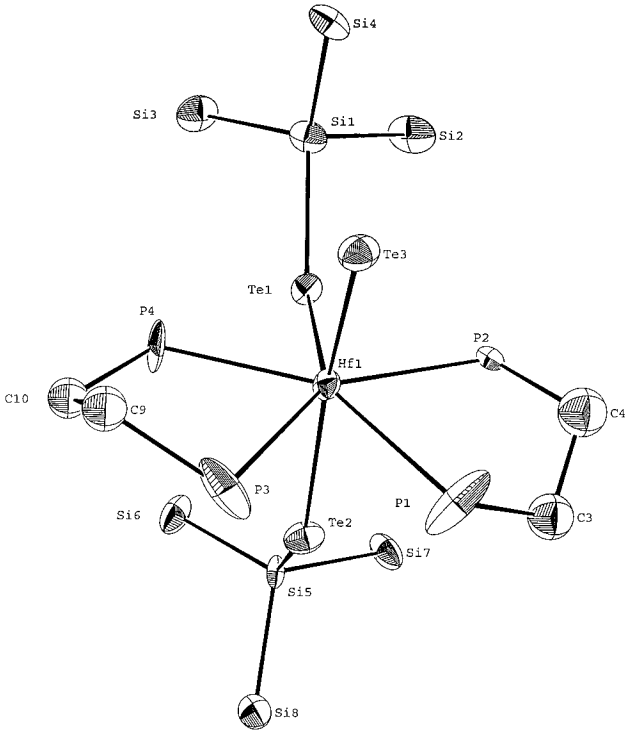

Figure 3. ORTEP view of the molecular structure of Hf[TeSi(SiMe$_3$)$_3$]$_2$(Te)(DMPE)$_2$. Methyl groups are omitted for clarity. Thermal ellipsoids are plotted at the 50% probability level.

complexes of $-$TeSi(SiMe$_3$)$_3$, no doubt for the minimization of steric interactions. The Hf$-$Te single bond lengths (3.019(1) and 2.918(2) Å) are significantly longer than the Hf$-$Te bond lengths in Hf[TeSi(SiMe$_3$)$_3$)]$_4$, a reflection of the increase in coordination number. In the zirconium complex, the Zr$-$Te single bonds are 2.939(1) and 3.028(1) Å as compared to the range of 2.724(1)$-$2.751(1) Å observed in Zr[TeSi(SiMe$_3$)$_3$]$_4$. In both molecules, it is the equitorial M$-$Te bond that is slightly longer, probably due to the trans influence of the two transoid phosphorus atoms. The longer M$-$Te single bonds in the seven-coordinate species compare well with the Zr$-$Te bond lengths in two independent molecules of Cp$_2$Zr(η^2-COMe)[TeSi(SiMe$_3$)$_3$] (2.990(1) and 2.996(1) Å), formally a nine-coordinate zirconium center. In comparison, the Hf$=$Te double bond is 2.637(2) Å, an average of 11% shorter than the Hf$-$Te single bonds; a similar contraction is observed in the zirconium complex (Zr$=$Te, 2.650(1) Å). These M$=$Te distances are slightly shorter than those reported for Cp$^{Et*}{}_2$M(Te)(NC$_5$H$_5$) (M $=$ Zr, Hf; Cp^{Et*} $=$ η^5-C$_5$Me$_4$Et) (Zr$=$Te, 2.729(1) Å;[40] Hf$=$Te, 2.716(1) Å [41]). In both sets of compounds, the Hf$=$Te bond lengths are slightly shorter than the Zr$=$Te distances.

The net tellurolate-to-telluride conversion is conveniently carried out in one step and is noteworthy in two respects: (i) the products are the only examples of a metal complex having both singly and doubly bonded tellurium in its coordination sphere, and (ii) the reactions may be viewed as homogenous solution state models for a first step in a chalcogenolate-to-chalcogenide transformation (eq 1). As observed by NMR spectroscopy, the chelating phosphine DMPM appears to form a similar species with the stoichiometry Zr[TeSi(SiMe$_3$)$_3$]$_2$(Te)(DMPM)$_2$; however, the compound is unstable with respect to further loss of Te[Si(SiMe$_3$)$_3$]$_2$, and a zirconium-containing product could not be isolated.

The increased steric demand of the $-$SeSi(SiMe$_3$)$_3$ ligand relative to the $-$TeSi(SiMe$_3$)$_3$ ligand is evidenced by a decreased affinity of the M[SeSi(SiMe$_3$)$_3$]$_4$ compounds (M $=$ Ti, Zr, Hf) toward Lewis bases. The selenolates do not form stable complexes with 1$-$2 equiv of phosphines (PMe$_3$, PMe$_2$Ph, PPh$_3$), isocyanides (CN(xylyl), CN(Bu^t), pyridine, or THF. Treatment with a large excess of Lewis base (e.g. 6 equiv of PMe$_3$), however, leads to elimination of Se[Si(SiMe$_3$)$_3$]$_2$ and formation of inseparable mixtures of metal-containing products.

Reaction of Zr[SeSi(SiMe$_3$)$_3$]$_4$ with 1 equiv of DMPE in hexanes or benzene resulted in the elimination of Se[Si(SiMe$_3$)$_3$]$_2$ and the precipitation of a bright red material with the stoichiometry Zr[SeSi(SiMe$_3$)$_3$]$_2$(Se)(DMPE).[42] Vibrational bands characteristic of the $-$SeSi(SiMe$_3$)$_3$ ligand are observed in the IR spectrum, and the compound reacts with excess H$_2$O, yielding HSeSi(SiMe$_3$)$_3$ and DMPE (2:1) (^{1}H NMR). Although the EI-MS shows an ion consistent with this formulation (m/z $=$ 974; correct isotope pattern), the presence of higher mass peaks may be evidence for oligomeric species. Indeed, the insolubility of the compound in common organic solvents (which has hampered further characterization) is also consistent with the latter suspicion. At this point we tentatively formulate the product as an oligomer with bridging Se and/or DMPE ligands. Hf[SeSi(SiMe$_3$)$_3$]$_4$ reacts with DMPE similarly to yield an orange product that was not investigated further.

As illustrated in eq 10, the reactions between M[SeSi(SiMe$_3$)$_3$]$_4$ (M $=$ Zr, Hf) and DMPM in hexanes lead to more tractable products. The Se- and DMPM-bridged dimers were

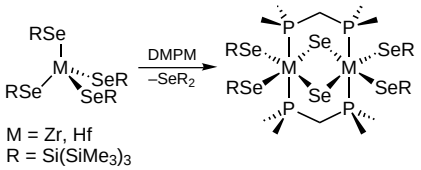

(10)

isolated in yields of 54% (Zr) and 23% (Hf) as red and orange crystals, respectively. The ^{77}Se NMR spectrum of the zirconium complex exhibits a resonance at δ 69 ($\Delta\nu_{1/2}$ $=$ 32 Hz) for the terminal selenolates and at δ 1390 ($\Delta\nu_{1/2}$ $=$ 40 Hz) for the bridging selenides.[43] The methylene hydrogens give rise to a pentet in the ^{1}H NMR spectrum that is indicative of a symmetrical A-frame complex.[44] A singlet with ^{77}Se satellites is observed in the ^{31}P{^{1}H} NMR spectrum at δ $-$23 ($^2J_{PSe}$ $=$ 11 Hz). While A-frame diphosphine coordination is well-documented for groups 5$-$10, we are not aware of any similarly bridged group 4 metals. Although the products formally arise by elimination of Se[Si(SiMe$_3$)$_3$]$_2$ and dimerization of the putative M[SeSi(SiMe$_3$)$_3$]$_2$(Se)(DMPM) intermediates, the propensity of DMPM to bridge rather than chelate[45] makes several dinuclear intermediates also feasible.

An ORTEP view of {Zr[SeSi(SiMe$_3$)$_3$]$_2$(μ-Se)(μ-DMPM)}$_2$ is given in Figure 4, and selected bond distances and bond angles are given in Table 4. The dimer lies on a crystallographic inversion center in the middle of the Zr$_2$Se$_2$ core. Two terminal $-$SeSi(SiMe$_3$)$_3$ ligands, two bridging Se atoms, and two P atoms of the bridging DMPM ligands are coordinated to each

(40) Howard, W. A.; Parkin, G. *J. Am. Chem. Soc.* **1994**, *116*, 606.
(41) Howard, W. A.; Parkin, G. *J. Organomet. Chem.* **1994**, *472*, C1.
(42) Reactions monitored by NMR spectroscopy prior to the precipitation of the product show significant Se[Si(SiMe$_3$)$_3$]$_2$ present but also at least three other uncharacterized products; this suggests that the reaction may be more complicated in nature than coordination of phosphine followed by elimination of selenoether.
(43) Due to limited solubility, only a resonance for the terminal selenolates at $-$60 ppm was detected in the hafnium analogue.
(44) Jenkins, J. A.; Cowie, M. *Organometallics* **1992**, *11*, 2774.
(45) Manojlovic-Muir, L.; Muir, K. W.; Frew, A. A.; Ling, S. S. M.; Thomson, M. A.; Puddephatt, R. J. *Organometallics* **1984**, *3*, 1637.

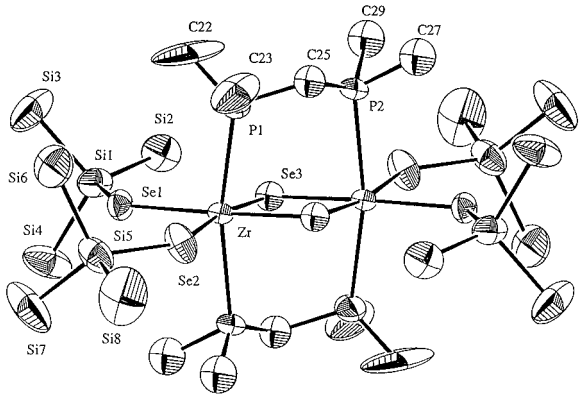

Figure 4. ORTEP view of the molecular structure of {Zr[SeSi(SiMe$_3$)$_3$]$_2$(μ-Se)(μ-DMPM)}$_2$. Methyl groups are omitted for clarity. Thermal ellipsoids are plotted at the 50% probability level.

Table 4. Selected Metrical Parameters for {Zr[SeSi(SiMe$_3$)$_3$]$_2$-(μ-Se)(μ-DMPM)}$_2$

Bond Distances (Å)			
Zr−Se1	2.636(2)	Zr−P1	2.749(5)
Zr−Se2	2.625(2)	Zr−P2	2.744(5)
Zr−Se3	2.598(4)	Se1−Si1	2.293(5)
Zr−Se3*	2.574(4)	Se2−Si5	2.277(6)
Zr−Zr*	3.628(3)		
Bond Angles (deg)			
Se1−Zr−Se2	92.10(7)	Zr−P1−C22	119.2(9)
Se1−Zr−Se3	93.4(1)	Zr−P1−C23	119(1)
Se2−Zr−Se3*	84.0(1)	Zr−Se1−Si1	129.0(2)
Se3−Zr−Se3*	90.9(1)	Zr−Se2−Si5	137.9(2)
P1−Zr−P2	166.9(2)		

zirconium. The average Zr−P bond distance of 2.746(7) Å is not unusual.[46] The terminal Zr−Se bonds are 2.636(2) and 2.625(2) Å, about 0.1 Å longer than in the four coordinate homoleptic selenolate. The Zr−Zr distance is 3.628(3) Å, and the P1−Zr−P2 angle is 166.9(2)°. Interestingly, the bulky silyl groups of the two terminal selenolate ligands are both folded about the zirconium in the same direction, and the tertiary silicon atoms are nearly coplanar with both the selenium atoms and the zirconium center (Se1−Zr−Se2−Si5 = 2.9(3)°; Se2−Zr−Se1−Si1 = 178.1(2)°). Disorder involving the bridging selenides (see below) precludes any meaningful discussion on the bond lengths and bond angles of the Zr_2Se_2 core. The core in Cp$_2$Ti(μ-Se)$_2$TiCp(Cl) is butterflied a total of 14.6°,[47] while those in [(^{t}BuCp)$_2$Zr(μ-E)]$_2$ (E = Se[48], Te[49,50]) are planar and nearly perfect squares.

Experimental Section

General. Standard inert atmosphere glovebox and Schlenk-line techniques were employed for all manipulations. All solvents were predried over 4 Å molecular sieves and in the case of benzene and hexanes were distilled from sodium/benzophenone under N_2, whereas toluene and hexamethyldisiloxane (HMDSO) were distilled from sodium. Solvents used for NMR spectroscopy were dried similarly and then vacuum-transferred prior to use. The compounds $ZrCl_4$ and $HfCl_4$ were purchased from commercial suppliers and were purified by vacuum sublimation. The compounds M(CH$_2$Ph)$_4$ (M = Ti,[35] Zr,[35] Hf[51]), TiCl$_3$(THF)$_3$,[52] Ti(CH$_2$Ph)$_2$(OEt)$_2$,[35] 1,2-bis(dimethylphosphino)-ethane (DMPE),[53] (THF)$_2$LiSeSi(SiMe$_3$)$_3$,[7] and HESi(SiMe$_3$)$_3$ (E = Se,[7] Te[54]) were prepared by literature procedures. The diphosphine 1,2-bis(dimethylphosphino)methane (DMPM) was purchased (Strem) and used as received.

All NMR spectra were recorded in C_6D_6 at room temperature unless otherwise noted. Chemical shifts (δ) for ^{1}H and ^{13}C{^{1}H} NMR spectra are reported relative to tetramethylsilane and were calibrated relative to the chemical shift of the residual protium (^{1}H) or the ^{13}C{^{1}H} signal of the solvent. ^{31}P{^{1}H} NMR spectra were externally referenced to 85% H_3PO_4 in H_2O. The ^{77}Se{^{1}H} NMR spectra were indirectly referenced to $SeMe_2$ at 0 ppm by direct reference to KSeCN (0.5 M in EtOH) at −322 ppm. Chemical shifts for ^{125}Te{^{1}H} NMR spectra are relative to $TeMe_2$ at 0 ppm by reference to external 1.74 M Te(OH)$_6$ in D_2O at δ 712 ppm. Samples for IR spectroscopy were prepared as Nujol mulls between CsI or KBr plates. Melting points were determined in sealed capillary tubes under nitrogen and are uncorrected. Samples for UV−vis spectroscopy were prepared as dilute hexanes solutions (ca. 10^{-3} M) in quartz cells under N_2. Elemental analyses and EI-MS measurements were performed within the College of Chemistry, University of California, Berkeley.

Ti[SeSi(SiMe$_3$)$_3$]$_4$·HMDSO. Hexanes (45 mL) was added to a mixture of TiCl$_3$(THF)$_3$ (0.361 g, 0.974 mmol) and (THF)$_2$LiSeSi-(SiMe$_3$)$_3$ (1.44 g, 3.01 mmol). The solution quickly took on a dark orange color that gradually intensified to dark red. After 12 h, the solvent was removed under reduced pressure and the deep red residue was extracted into warm HMDSO (50 mL). The mixture was concentrated and cooled to −35 °C for 12 h. The product was collected by filtration as black crystals; 0.56 g, 39% on Ti (mp 261−263 °C (dec)). IR: 1256 m, 1243 s, 859 s, 838 vs, 723 m, 689 m, 623 m cm^{-1}. ^{1}H NMR (300 MHz): δ 0.50 (s, 108H), 0.11 (s, 18H). ^{13}C{^{1}H} NMR (100 MHz): δ 1.86 (s), 2.02 (s, HMDSO). ^{77}Se{^{1}H} NMR (57.24 MHz): δ 865 (s). UV−vis (hexane, nm): λ_{max} 208, 340, 498, 640. Anal. Calcd for $C_{42}H_{126}OSe_4Si_{18}Ti$: C, 33.26; H, 8.37. Found: C, 33.38; H, 8.45.

Ti[TeSi(SiMe$_3$)$_3$]$_4$. A hexanes solution (40 mL) of (THF)$_2$LiTeSi-(SiMe$_3$)$_3$ (1.83 g, 3.48 mmol) was added to a cold (−20 °C) suspension of TiCl$_3$(THF)$_3$ (0.429 g, 1.16 mmol) in hexanes (20 mL). The mixture was warmed to room temperature over 2 h and became an intense cranberry red. The volatiles were removed under reduced pressure and the red-purple solid was extracted into hexanes (2 × 30 mL). The deep red filtrate was concentrated to 10 mL and cooled to −35 °C for 24 h. Black crystals were isolated by filtration; 606 mg, 34% on Ti (mp 230−232 °C (dec.). IR: 1460 s, 1377 m, 1242 m, 837 vs, br, 729 w, br, 688 w, 621 w, 478 w cm^{-1}. ^{1}H NMR (300 MHz): δ 0.54 (s). ^{13}C{^{1}H} NMR (100 MHz): δ 2.68 (s). ^{125}Te{^{1}H} NMR (157.77 MHz): δ 1302 (s). Anal. Calcd for $C_{36}H_{108}Si_{16}Te_4Ti$: C, 27.92; H, 7.03. Found: C, 27.85; H, 6.91.

Zr[SeSi(SiMe$_3$)$_3$]$_4$. Method A. Hexanes (40 mL) was added to a mixture of $ZrCl_4$ (0.250 g, 1.07 mmol) and (THF)$_2$LiSeSi(SiMe$_3$)$_3$ (2.10 g, 4.40 mmol), and the resulting light orange solution was stirred at room temperature for 12 h, gradually darkening to orange-red. The solvent was removed under reduced pressure and the residue extracted into HMDSO (2 × 20 mL). Concentration of this solution followed by cooling to −35 °C gave the product as an orange solid that was separated by filtration (0.730 g, 49%).

Method B. Hexanes (50 mL) was added to a mixture of Zr(CH$_2$-Ph)$_4$ (0.584 g, 1.28 mmol) and HSeSi(SiMe$_3$)$_3$ (1.68 g, 5.13 mmol), and the solution was heated to reflux for 6 h. The solvent was removed under reduced pressure and the orange solid dissolved in HMDSO (40 mL). The solution was filtered, concentrated to 10 mL, and cooled to −35 °C for 12 h. The product was collected by filtration as opaque, orange crystals; 1.32 g, 74% (mp 268−269 °C (dec.), black). IR: 1258 m, 1243 s, 861 s, 838 vs, 688 m 622 m cm^{-1}. ^{1}H NMR (300 MHz): δ 0.48 (s). ^{13}C{^{1}H} NMR (100 MHz): δ 1.50 (s). ^{77}Se{^{1}H} NMR

(46) Girolami, G. S.; Wilkinson, G. *J. Chem. Soc., Dalton Trans.* **1984**, 2789.
(47) Fenske, D.; Maue, P. G. *Z. Naturforsch.* **1988**, *43b*, 1213.
(48) Tainturier, G.; Fahim, M.; Gautheron, B. *J. Organomet. Chem.* **1989**, 311.
(49) Erker, G.; Muhlenbernd, T.; Nolte, R.; Petersen, J. L.; Tainturier, G.; Gautheron, B. *J. Organomet. Chem.* **1986**, *314*, C21.
(50) Erker, G.; Nolte, R.; Tainturier, G.; Rheingold, A. *Organometallics* **1989**, *8*, 454.
(51) Felten, J. J.; Anderson, W. P. *J. Organomet. Chem.* **1972**, *36*, 87.
(52) Manzer, L. E.; Deaton, J.; Sharp, P.; Schrock, R. R. *Inorg. Synth.* **1982**, *21*, 137.
(53) Burt, R. J.; Chatt, J.; Hussain, W.; Leigh, G. J. *J. Organomet. Chem.* **1979**, *182*, 203.
(54) Dabbousi, B. O.; Bonasia, P. J.; Arnold, J. *J. Am. Chem. Soc.* **1991**, *113*, 3186.

(57.24 MHz): δ 356 (s). UV−vis (nm): λ_{max} 216, 286, 346, 458. Anal. Calcd for $C_{36}H_{108}Se_4Si_{16}Zr$: C, 30.94; H, 7.79. Found: C, 30.99; H, 7.56.

Zr[TeSi(SiMe$_3$)$_3$]$_4$. A hexanes solution (50 mL) of HTeSi(SiMe$_3$)$_3$ (4.95 g, 13.2 mmol) was added to a cold (−20 °C) suspension of Zr(CH$_2$Ph)$_4$ (1.50 g, 3.29 mmol) in hexanes (50 mL). The mixture was warmed to room temperature and stirred for 4 h. The solvent was removed under reduced pressure, and the green, microcrystalline solid was recrystallized from hexanes affording the product in two crops; 4.05 g, 77% (mp 227−230 °C (dec.), black). IR: 1256 sh, 1243 s, 837 vs, br, 744 w, 688 m, 622 m cm^{-1}. ^{1}H NMR (400 MHz): δ 0.51 (s). ^{13}C{^{1}H} NMR (100 MHz): δ 2.39 (s). ^{125}Te{^{1}H} NMR (157.77 MHz): δ 459 (s). EI-MS: 1592 (M$^+$), 1344, 1215, 895, 752, 679, 623. Anal. Calcd for $C_{36}H_{108}Si_{16}Te_4Zr$: C, 27.16; H, 6.84. Found: C, 26.96; H, 6.75.

Hf[SeSi(SiMe$_3$)$_3$]$_4$. This preparation was analogous to that used to synthesize the zirconium complex by method A; 0.67 g, 48% (mp 262−264 °C (dec.), black). IR: 1258 m, 1244 m, 861 m, 838 s, 688 m, 622 m cm^{-1}. ^{1}H NMR (400 MHz): δ 0.49 (s). ^{13}C{^{1}H} NMR (100 MHz): δ 1.55 (s). ^{77}Se{^{1}H} NMR (57.24 MHz): δ 211 (s). UV−vis (nm): λ_{max} 216, 280 sh, 406. Anal. Calcd for $C_{36}H_{108}HfSe_4Si_{16}$: C, 29.12; H, 7.33. Found: C, 29.46; H, 7.18.

Hf[TeSi(SiMe$_3$)$_3$]$_4$. This preparation was analogous to that used for the zirconium complex; 0.40 g, 79% (mp 225−230 °C (dec.)). IR: 1257 w, 1243 s, 858 sh, 836 vs, br, 688 m, 622 m cm^{-1}. ^{1}H NMR (400 MHz): δ 0.51 (s). ^{13}C{^{1}H} NMR (100 MHz): δ 2.50 (s). ^{125}Te{^{1}H} NMR (157.77 MHz): δ 193 (s). EI-MS: 1680 (M$^+$), 1433, 1303, 982, 927, 623. Anal. Calcd for $C_{36}H_{108}Si_{16}Te_4Hf$: C, 25.79; H, 6.48. Found: C, 25.39; H, 6.49.

Generation of Ti[SeSi(SiMe$_3$)$_3$]$_2$(OEt)$_2$. A C_7D_8 solution (0.5 mL) containing 31.2 mg (0.0974 mmol) of Ti(CH$_2$Ph)$_2$(OEt)$_2$ and 63.8 mg (0.195 mmol) of HSeSi(SiMe$_3$)$_3$ was prepared and loaded into a NMR tube fitted with a sealable Teflon cap. The clear orange solution was heated to 50 °C for 14 h and became a cherry red color. Analysis of the sample by NMR spectroscopy indicated the formation of toluene and Ti[SeSi(SiMe$_3$)$_3$]$_2$(OEt)$_2$; 95%. ^{1}H NMR (300 MHz): δ 0.40 (s, 54H, SiMe$_3$), 1.23 (t, 6H, OCh$_2$C*H*$_3$, 7 Hz), 4.34 (q, 4H, OC*H*$_2$CH$_3$, 7 Hz). ^{13}C{^{1}H} NMR (100 MHz): δ 1.10 (s, SiMe$_3$), 21.4 (s, OCH$_2$*C*H$_3$), 76.1 (s, *C*H$_2$CH$_3$). ^{77}Se{^{1}H} NMR (57.24 MHz): δ 416 (s).

Ti[SeSi(SiMe$_3$)$_3$]$_3$(CH$_2$Ph). A hexanes solution (15 mL) of HSeSi(SiMe$_3$)$_3$ (1.27 g, 3.88 mmol) was added to a cold (−5 °C) suspension of Ti(CH$_2$Ph)$_4$ (0.535 g, 1.30 mmol) in hexanes (40 mL). The mixture was warmed to room temperature and stirred for 1 h during which time it became increasingly red. The solvent was removed under reduced pressure and the red precipitate extracted into HMDSO (35 mL). Concentration and cooling of this solution afforded the product in two crops as a rust colored, microcrystalline solid; 0.86 g, 59% (mp 174−176 °C (dec.), black). IR: 1256 w, 1243 m, 859 m, 835s, 740 w, 722 w, 689 w cm^{-1}. ^{1}H NMR (400 MHz): δ 0.44 (s, 81H, SiMe$_3$), 3.58 (s, 2H, C*H*$_2$Ph), 6.85 (t, 1H, *p*-Ph, 7 Hz), 7.22 (t, H, *m*-Ph, 8 Hz), 7.56 (d, 2H, *o*-Ph, 7 Hz). ^{13}C{^{1}H} NMR (100 MHz): δ 1.46 (s, SiMe$_3$), 109.56 (s, *C*H$_2$Ph), 148.50, 130.12, 128.37, 123.24 (s, Ph). ^{77}Se{^{1}H} NMR (57.24 MHz): δ 828 (s). Uv−vis (nm): λ_{max} 208, 250, 320, 430. Anal. Calcd for $C_{34}H_{88}Se_3Si_{16}Ti$: C, 36.5; H, 7.93. Found: C, 36.2; H, 8.19.

Zr[SeSi(SiMe$_3$)$_3$]$_3$(CH$_2$Ph). This preparation was analogous with that used to synthesize the titanium derivative; 1.6 g, 54% (mp 172−174 °C (dec.), black). The bright orange product obtained is usually contaminated with ca. 5% of Zr[SeSi(SiMe$_3$)$_3$]$_4$ (^{1}H NMR). Attempts to purify the compound further were unsuccessful (mp 172−174 °C (dec.)). IR: 1257 w, 1242 m, 860 m, 838 s, 740 w, 723 w, 691 w, 622 w cm^{-1}. ^{1}H NMR (400 MHz): δ 0.41 (s, 81H, SiMe$_3$), 3.10 (s, 2H, C*H*$_2$Ph), 7.08 (t, 1H, *p*-Ph, 6 Hz), 7.22 (t, 3H, *m*-Ph, 6 Hz), 7.33 (d, 2H, *o*-Ph, 6 Hz). ^{13}C{^{1}H} NMR (100 MHz): δ 1.40 (s, SiMe$_3$), 83.12 (s, *C*H$_2$Ph), 137.43, 131.21, 130.82, 125.68 (s, Ph). ^{77}Se{^{1}H} NMR (57.24 MHz): δ 338 (s). Uv−vis (nm): λ_{max} 210, 262, 336.

Hf[SeSi(SiMe$_3$)$_3$]$_3$(CH$_2$Ph). A hexanes solution (15 mL) of HSeSi(SiMe$_3$)$_3$ (2.55 g, 7.78 mmol) was added dropwise over 10 min to a stirred hexanes solution (50 mL) of Hf(CH$_2$Ph)$_4$ (1.41 g, 2.60 mmol). The mixture gradually became pale, yellow-green. After 1 h, the solvent was removed under reduced pressure, leaving the product as a pastel yellow, microcrystalline solid; 3.02 g, 93% (mp 172−178 °C (dec.), orange-red oil). IR: 1258 w, 1244 m, 862 m, 837 s, 741 w, 723 w, 691 w, 622 w cm^{-1}. ^{1}H NMR (300 MHz): δ 0.41 (s, 81H, SiMe$_3$), 2.69 (s, 2H, C*H*$_2$Ph), 6.92 (t, 1H, *p*-Ph, 7 Hz), 7.25 (t, 3H, *m*-Ph, 8 Hz), 7.50 (d, 2H, *o*-Ph, 6 Hz). ^{13}C{^{1}H} NMR (100 MHz): δ 1.30 (s, SiMe$_3$), 97.54 (s, *C*H$_2$Ph), 142.12, 130.33, 128.89, 123.57 (s, Ph). ^{77}Se{^{1}H} NMR (57.24 MHz): δ 206 (s). Uv−vis (nm): λ_{max} 214, 246, 304. Anal. Calcd for $C_{34}H_{88}HfSe_3Si_{16}$: C, 32.68; H, 7.10. Found: C, 32.31; H, 7.37.

Zr[TeSi(SiMe$_3$)$_3$]$_4$(CN(xylyl))$_2$. A hexanes solution (30 mL) of xylyl isocyanide (155 mg, 1.18 mmol) was added to a hexanes solution (30 mL) of Zr[TeSi(SiMe$_3$)$_3$]$_4$ (0.94 g, 59 mmol). The gree mixture immediately became intensely purple. After stirring for 0.5 h, the volatiles were removed under reduced pressure and the solid extracted into and recrystallized from hexanes at −35 °C. The product was isolated in two crops by filtration as a maroon, microcrystalline solid; 0.77 g, 70% (mp 145−148 °C (dec.)). IR: 2151 (ν_{CN}), 1236 w, 835 s, br, 771 w, 689 w, 620 w cm^{-1}. ^{1}H NMR (400 MHz): δ 0.48 (s, 108H, SiMe$_3$), 2.70 (s, 12H, xylyl-Me), 6.77 (d, 4H, *m*-Ph), 6.89 (t, 2H, *p*-Ph). ^{13}C{^{1}H} NMR (100 MHz, C_7D_8): δ 3.00 (s, SiMe$_3$), 20.01 (s, xylyl-Me), 135.26, 129.76, 128.31, 127.09 (s, Ph), 173.5 (s, xylyl-N*C*). ^{125}Te{^{1}H} NMR (157.77 MHz, C_7D_8): δ 203 (s). EI-MS: 1592 (M$^+$ − 2C$_6$H$_3$Me$_2$NC), 1346, 1216. Anal. Calcd for $C_{54}H_{126}N_2Si_{16}Te_4Zr$: C, 35.0; H, 6.85; N, 1.51. Found: C, 35.3; H, 6.65; N, 1.52.

Hf[TeSi(SiMe$_3$)$_3$]$_4$(CN(xylyl))$_2$. This preparation was analogous with that used for the zirconium analogue except the reaction was stirred for 10 h; 0.43 g, 49% (dark red, (mp 157−163 °C (dec.)). IR: 2153 (ν_{CN}), 1240 s, 1174 w, 1092 w, 1034 w, 860 sh, 837 vs, br, 775 m, 688 m, 624 m cm^{-1}. ^{1}H NMR (400 MHz): δ 0.50 (s, 108H, SiMe$_3$), 2.72 (s, 12H, xylyl-Me), 6.75 (d, 4H, *m*-Ph), 6.88 (t, 2H, *p*-Ph). ^{13}C{^{1}H} NMR (100 MHz, C_7D_8): δ 3.04 (s, SiMe$_3$), 20.01 (s, xylyl-Me), 135.33, 129.81, 128.34, 126.96 (s, Ph), 178.5 (s, xylyl-N*C*). ^{125}Te{^{1}H} NMR (157.77 MHz, C_7D_8): δ −14 (s). Anal. Calcd for $C_{54}H_{126}HfN_2Si_{16}Te_4$: C, 33.4; H, 6.54; N, 1.44. Found: C, 31.6; H, 6.46; N, 1.39.

Zr[TeSi(SiMe$_3$)$_3$]$_4$(DMPE). DMPE (105 μL, 0.628 mmol) was added to a hexanes solution (50 mL) of Zr[TeSi(SiMe$_3$)$_3$]$_4$ (1.00 g, 0.628 mmol). The red-purple mixture was stirred for 8 h. Concentration and cooling of the mother liquor to −78 °C afforded the maroon product that was isolated by filtration; 0.62 g, 57% (mp 176−178 °C (dec.)). IR: 1242 s, 947 w, 929 w, 858 sh, 835 s, br, 722 w, 688 w, 624 w cm^{-1}. ^{1}H NMR (400 MHz): δ 0.48 (s, 54H, SiMe$_3$), 0.62 (s, 54H, SiMe$_3$), 1.63 (m, 4H, PCH$_2$), 1.76 (m, 12H, PMe). ^{13}C{^{1}H} NMR (100 MHz, C_7D_8): δ 3.59 (s, SiMe$_3$), 3.63 (s, SiMe$_3$), 22.33 (m, PCH$_3$), 27.90 (m, PCH$_2$). ^{31}P{^{1}H} NMR (162.92 MHz, C_7D_8): δ −2.92 (s). ^{125}Te{^{1}H} NMR (157.77 MHz, C_7D_8): δ 151 (s), −116 (s).

Hf[TeSi(SiMe$_3$)$_3$]$_4$(DMPE). This preparation was analogous with that used for the zirconium analogue; 250 mg, 46% (bronze colored). ^{1}H NMR (400 MHz): δ 0.48 (s, 54H, SiMe$_3$), 0.60 (s, 54H, SiMe$_3$), 1.68 (m, 4H, PCH$_2$), 1.81 (m, 12H, PMe). ^{13}C{^{1}H} NMR (100 MHz, C_7D_8): δ 2.40 (s, SiMe$_3$), 3.67 (s, SiMe$_3$), 22.38 (m, PCH$_3$), 27.94 (m, PCH$_2$). ^{31}P{^{1}H} NMR (161.92 MHz, C_7D_8): δ −3.36 (s). ^{125}Te{^{1}H} NMR (157.77 MHz, C_7D_8): δ 128 (s), −349 (s). The extreme solubility of both the zirconium and hafnium mono(DPME) adducts in hexane, pentane, and hexamethyldisiloxane prevented purification to >95%. Characterization rests upon NMR data and the smooth conversion to the bis(DMPE) tellurides upon addition of 1 equiv of DMPE.

Zr[TeSi(SiMe$_3$)$_3$]$_2$(Te)(DMPE)$_2$. DMPE (0.36 mL, 4.38 mmol) was added to a hexanes solution (30 mL) of Zr[TeSi(SiMe$_3$)$_3$]$_4$ (3.49 g, 2.19 mmol). The initially green solution changed to purple and then to brown. The mixture was stirred for 0.5 h, concentrated, and then cooled to −35 °C. Red-brown crystals were separated from the mother liquor by filtration; 2.39g, 86% (mp 128−130 °C (dec.)). IR: 1239 m, 945 m, 930 m, 890 w, 835 vs, br, 727 w, 686 w, 647 w, 623 w cm^{-1}. ^{1}H NMR (400 MHz, C_7D_8, −78 °C): δ 0.32 (s, 27H, SiMe$_3$), 0.58 (s, 27H, SiMe$_3$), 1.24 (m, 12H, PMe), 1.58 (m, 12H, PMe), 2.05 (m, 4H, PCH$_2$), 2.19 (m, 4H, PCH$_2$). ^{31}P{^{1}H} NMR (161.92 MHz, C_7D_8, −80 °C): δ 1.28 (s, $^2J_{PTe}$ = 74 Hz), −3.22 (s, $^2J_{PTe}$ = 168 Hz). ^{125}Te{^{1}H} NMR (157.77 MHz, C_7D_8, −78 °C): δ −706 (s), −1173 (t, $^2J_{TeP}$ = 166 Hz), −1197 (s). Anal. Calcd for $C_{30}H_{86}P_4Si_8Te_3Zr$: C, 32.6; H, 6.96. Found: C, 32.8; H, 6.97.

Hf[TeSi(SiMe$_3$)$_3$]$_2$(Te)(DMPE)$_2$. This preparation was analogous to that used to synthesize the zirconium analogue; 222 mg, 55% (red-

Table 5. Summary of X-ray Diffraction Data

	$Zr[SeSi(SiMe_3)_3]_4$	$Hf[TeSi(SiMe_3)_3]_4$	$Hf[TeSi(SiMe_3)_3]_2(Te)(DMPE)_2$	$\{Zr[SeSi(SiMe_3)_3]_2(Se)(DMPM)\}_2$
formula	$C_{36}H_{108}Se_4Si_{16}Zr$	$C_{36}H_{108}HfSi_{16}Te_4$	$C_{30}H_{86}HfP_4Si_8Te_3$	$C_{46}H_{136}P_4Se_6Si_{16}Zr_2$
MW	1397.68	1679.53	1356.89	1919.05
space group	$P2_1/c$	$P2_1/c$	$P2_1$	$P2_1/n$
a (Å)	22.6944(34)	22.494(5)	14.795(3)	14.7651(13)
b (Å)	15.2943(55)	15.609(5)	14.289(3)	18.8579(17)
c (Å)	22.7758(61)	22.742(5)	15.4212(2)	18.6072(17)
α (deg)	90	90	90	90
β (deg)	105.695(17)	104.480(5)	102.543(3)	111.031(1)
γ (deg)	90	90	90	90
vol (Å^3)	7611(4)	7731	3182(1)	4836(1)
Z	4	4	2	2
d_{calcd} (g cm^{-3})	1.22	1.443	1.416	1.32
cryst size (mm)	0.50 × 0.50 × 0.40	0.20 × 0.15 × 0.10	0.30 × 0.20 × 0.10	0.18 × 0.13 × 0.04
radiation (λ/Å)	Mo Kα (0.7103)	Mo Kα (0.7103)	Mo Kα (0.7103)	Mo Kα (0.7103)
scan mode	$\theta-2\theta$	$\theta-2\theta$	$\theta-2\theta$	ω (0.3 deg scans)
2θ range (deg)	3−45	3−45	3−45	4−46.5
collcn range	$+h, +k, \pm l$	$+h, +k, \pm l$	$+h, +k, \pm l$	hemisphere
absorption coeff, μ (cm^{-1})	23.31	30.9	32.4	27.6
no. of unique reflcns	10402	10082	4354	6969
reflcns with $F^2 > 3\sigma(F^2)$	5300	7019	3403	3480
final R,R_w	0.0529, 0.0369	0.0448, 0.0545	0.0478, 0.0670	0.0826, 0.0813
T (°C)	−85	−93	−105	−94

brown). ^{1}H NMR (400 MHz, C_7D_8, −78 °C): δ 0.36 (s, 27H, $SiMe_3$), 0.64 (s, 27H, $SiMe_3$), 1.36 (m, 12H, PMe_3), 1.64 (m, 12H, PMe_3), 2.05 (m, 4H, PCH_2), 2.12 (m, 4H, PCH_2). $^{31}P\{^1H\}$ NMR (161.92 MHz, −78 °C): δ −1.39 (s, br), −10.67 (s, br). $^{125}Te\{^1H\}$ NMR (157.77 MHz, C_7D_8, −78 °C): δ −701 (s), −1212 (t, $^2J_{TeP}$ = 190 Hz), −1250 (s).

{Zr[SeSi(SiMe$_3$)$_3$]$_2$(Se)(DMPE)}$_n$. DMPE (15 μL, 0.090 mmol) was added to a hexanes solution (10 mL) of $Zr[SeSi(SiMe_3)_3]_4$ (114 mg, 0.0816 mmol). The solution was thoroughly mixed and allowed to remain undisturbed at room temperature. After 24 h, red crystals were isolated by filtration; 0.49 mg, 62% (mp 185−186 °C (dec.), black). IR: 1295 w, 1280 w, 1257 w, 1240 m, 946 m, 935 m, 920 w sh, 896 w, 863 s, 835 vs, 687 m, 649 w, 626 m, 462 w cm^{-1}. EI-MS: 974 (M^+ for monomer). Anal. Calcd for $C_{24}H_{70}Se_3Si_8P_2Zr$: C, 30.07; H, 6.74. Found: C, 29.84; H, 6.94.

{Zr[SeSi(SiMe$_3$)$_3$]$_2$(μ-Se)(μ-DMPM)}$_2$. A hexanes solution (20 mL) of $Zr[SeSi(SiMe_3)_3]_4$ (331 mg, 0.224 mmol) was treated with DMPM (35 μL, 0.22 mmol) and the mixture stirred for 24 h, becoming increasingly red. The solvent was removed under reduced pressure and the red-orange residue extracted with hexanes (2 × 15 mL). Concentration of the red filtrate and cooling to −35 °C afforded the product as red crystals that were isolated by filtration; 105 mg, 54% (mp 175−180 °C (dec.), black). IR: 1297 w, 1283 w, 1256 w, 1239 m, 946 m, 933 m, 893 m, 860 m, 834 s, 686 m, 622 m cm^{-1}. ^{1}H NMR (400 MHz, C_7D_8): δ 0.47 (s, 54H, $SiMe_3$), 1.56 (s, 12H, PMe), 1.91 (pentet, 2H, PCH_2, J_{HP} = 5 Hz). $^{13}C\{^1H\}$ NMR (100 MHz, C_7D_8): δ 2.28 (s, $SiMe_3$), 18.5 (m, PMe). $^{31}P\{^1H\}$ NMR (161.92 MHz, C_7D_8): δ −23.3 (s, J_{PSe} = 11 Hz). $^{77}Se\{^1H\}$ NMR (57.24 MHz, C_7D_8): δ 63 (s, $\Delta\nu_{1/2}$ = 32 Hz, terminal selenolate), 1390 (s, $\Delta\nu_{1/2}$ = 40 Hz, μ-Se). Anal. Calcd for $C_{46}H_{136}P_4Se_6Si_{16}Zr_2$: C, 28.79; H, 7.14. Found: C, 28.53; H, 7.29.

{Hf[SeSi(SiMe$_3$)$_3$]$_2$(μ-Se)(μ-DMPM)}$_2$. This preparation was analogous with that used to prepare the analogous zirconium derivative except the reaction was stirred a total of 48 h; 80 mg, 23% (mp 200−215 °C (dec.), orange > red > black). ^{1}H NMR (300 MHz): δ 0.50 (s, 54H, $SiMe_3$), 1.65 (s, 12H, PMe), 2.06 (pentet, 2H, PCH_2, J_{HP} = 5 Hz). $^{13}C\{^1H\}$ NMR (100 MHz): δ 2.39 (s, $SiMe_3$), 18.6 (m, PMe). $^{31}P\{^1H\}$ NMR (162 MHz): δ −20.7 (s, $^2J_{PSe}$ = 13 Hz). ^{77}Se NMR (57.2 MHz, C_7D_8): δ −60 (s, terminal selenolate, $\Delta\nu_{1/2}$ = 30 Hz). Due to limited solubility (ca. 10 mg·mL^{-1}), a resonance for the μ-Se could not be detected. Anal. Calcd for $C_{46}H_{136}Hf_2P_4Se_6Si_{16}$: C, 26.39; H, 6.55. Found: C, 26.14; H, 6.79.

X-ray Crystallography. A summary of the data collection parameters and structural refinement for all crystallographically characterized compounds is given in Table 5.

Zr[SeSi(SiMe$_3$)$_3$]$_4$. Suitable crystals were grown by slowly cooling a saturated hexanes solution of the compound to −35 °C. The crystal was mounted on a glass capillary with Paratone-N oil, transferred to a CAD4 diffractometer, and centered in a steam of cold dinitrogen gas. Cell constants and orientation matrix were obtained from the least squares refinement of 25 carefully centered high-angle reflections. The intensities of three standard reflections were measured every 200 reflections, and no crystal decay was observed over the course of the experiment. The data were corrected for Lorentz and polarization effects. An empirical absorption correction based on azimuthal scans near χ = 90° was applied to the data. Inspection of the systematic absences uniquely defined the space group $P2_1/c$. The structure was solved by direct methods using the TEXSAN package[55] on a Digital VAX station and refined using standard least squares and Fourier techniques. The silicons Si14−Si16 (attached to Si13) were each disordered about two sites and were modeled by assinging them occupancies of 0.5. Two of the carbons for each disordered $-SiMe_3$ were in the same position, and the remaining carbon atoms were given occupancies of 0.5. The partial occupancy atoms refined successfully with isotropic thermal parameters. All of the other non-hydrogen atoms were refined with anisotropic thermal parameters. All of the hydrogen atoms except those associated with the disordered $-Si(SiMe_3)_3$ were introduced at idealized positions and included in structure factor calculations but not refined. Neutral atomic scattering factors were taken from Cromer and Waber,[56] and anomalous dispersion effects were included in F_c.[57] The final residuals for 508 variables refined against 5300 data for which $F^2 > 3\sigma(F^2)$ were R = 0.0529, R_w = 0.0369, and GOF = 2.16.

Hf[TeSi(SiMe$_3$)$_3$]$_4$. Crystals were grown from hexanes at −35 °C. Unit cell parameters, orientation matrix, and diffraction data were collected with an Enraf-Nonius CAD-4-diffractometer as above. The structure was solved by direct methods (SHELXS) and refined via standard least squares and Fourier techniques.[58,59] All non-hydrogen atoms were refined with anisotropic thermal parameters. Hydrogen atoms were treated as above. The final residuals for 515 variables refined against 7019 data for which $F^2 > 3\sigma(F^2)$ were R = 0.0448, R_w = 0.0545, and GOF = 1.31.

Hf[TeSi(SiMe$_3$)$_3$]$_2$(Te)(DMPE)$_2$. Crystals were grown from pentane at −35 °C. Diffraction data were collected as described above. The

(55) *TEXSAN*: *Crystal Structure Analysis Package*; Molecular Structure Corp.: 1992.
(56) Cromer, D. T.; Waber, J. T. *International Tables for X-ray Crystallography*; The Kynoch Press: Birmingham, England, 1974; Vol. IV, Table 2.2B.
(57) Cromer, D. T.; Waber, J. T. *International Tables for X-ray Crystallography*; The Kynoch Press: Birmingham, England, 1974; Vol. IV, Table 2.3.1.
(58) Calculations were performed on a DEC Microvax II using locally modified versions of the Enraf-Nonius MolEN structure solution and refinement package and other programs.
(59) *MolEn*; Delft Instruments: Delft, The Netherlands, 1990.

structure was solved by direct methods (SHELXS) and refined as above. An empirical absorption correction was applied using DIFABS.[60−62] A carbon atom on a $-SiMe_3$ was disordered about two sites and modeled successfully with two partial occupancy carbon atoms (C21, 0.65 occ; C21′, 0.35 occ). All carbon atoms were refined with isotropic thermal parameters and all remaining heavy atoms with anisotropic thermal parameters. The final residuals for 268 variables refined against 3403 data for which $F^2 > 3\sigma(F^2)$ were $R = 0.0478$, $R_w = 0.0670$, and GOF = 2.75.

{Zr[SeSi(SiMe$_3$)$_3$]$_2$(μ-Se)(μ-DMPM)}$_2$. A suitable crystal was grown from a concentrated hexanes solution at −35 °C. Data collection was conducted with a Siemens SMART diffractometer/CCD area detector.[63] A preliminary orientation matrix and unit cell parameters were determined by collecting 60 10-s frames, followed by spot integration and least squares refinement. A hemisphere of data was collected using 30-s scans per frame. The raw data were integrated (*XY* spot spread = 1.60°; *Z* spot spread = 0.60°) and the unit cell parameters refined (3290 reflections with $I > 10\sigma$) using SAINT.[64] Preliminary data analysis and an absorption correction ($T_{min} = 0.521$; $T_{max} = 0.887$) were performed using XPREP.[65] Of the 11564 reflections measured, 6969 were independent and the redundant reflections were averaged with an 8.42% internal consistency. No correction for crystal decay was applied. The structure was solved and refined as for Zr[SeSi(SiMe$_3$)$_3$]$_4$. The molecule lies on a crystallographic inversion center in the center of the Zr_2Se_2 core. Three carbon atoms of the peripheral $-SiMe_3$ groups were disordered about two sites and were modeled as six carbons with occupancies of 0.5. The methylene bridge of the DMPM, the pair of methyl carbons off P2, and the bridging Se atoms were similarly disordered and modeled analogously. All partial occupancy atoms refined successfully with isotropic thermal parameters. Methyl hydrogens were introduced at fixed positions for all full occupancy carbons and treated as above. The final residuals for 327 variables refined against 3480 data for which $F^2 > 3\sigma(F^2)$ were $R = 0.0826$, $R_w = 0.0813$, and GOF = 2.55.

Acknowledgment. We are grateful to the National Science Foundation for financial support, the Alfred P. Sloan Foundation for the award of a research fellowship to J.A., and to E. K. Brady for preliminary experiments.

Supporting Information Available: ORTEP diagrams showing complete numbering schemes and listings of bond distances and angles and positional and thermal parameters, for Hf[TeSi(SiMe$_3$)$_3$]$_4$, Zr[SeSi(SiMe$_3$)$_3$]$_4$, Hf[TeSi(SiMe$_3$)$_3$]$_2$(Te)(DMPE)$_2$, and {Zr[SeSi(SiMe$_3$)$_3$]$_2$(μ-Se)(μ-η^2-DMPM)$_2$}$_2$ (25 pages). Ordering information is given on any current masthead page.

IC9600689

(60) Katayama, C.; Sakabe, N.; Sakabe, K. *Acta Crystallogr*. **1972**, *A39*, 158.
(61) Ugozzli, F. *Comput*. *Chem*. **1987**, *11*, 109.
(62) Katayama, C. *Acta Crystallogr*. **1986**, *A42*, 19.
(63) *SMART Area-Detector Software Package*; Siemens Industrial Automation, Inc.: Madison, WI, 1993.
(64) *SAINT*: *SAX Area-Detector Integration Program*, v. 4.024; Siemens Industrial Automation, Inc.: Madison, WI, 1994.
(65) *XPREP*: *Part of the SHELXTL Crystal Structure Determination Package*; Siemens Industrial Automation: Madison, WI, 1994.